

Soil porous system changes quantified by analyzing soil water retention curve modifications

Luiz F. Pires^{a,*}, Fabio A.M. Cássaro^a, Klaus Reichardt^b, Osny O.S. Bacchi^b

^a Department of Physics, State University of Ponta Grossa, UEPG, C.E.P. 84.030-900 Ponta Grossa, PR, Brazil

^b Center for Nuclear Energy in Agriculture, USP/CENA, C.P. 96, C.E.P. 13.400-970 Piracicaba, SP, Brazil

ARTICLE INFO

Article history:

Received 3 August 2007

Received in revised form 2 April 2008

Accepted 18 April 2008

Keywords:

Wetting and drying cycles

Soil structure

S-theory

Pore size distribution

Log-normal distribution

ABSTRACT

Soil water retention curves (SWRCs) relate soil water pressure head (h) to soil water content (θ) and can also be used to find information regarding soil pore distribution. To analyze SWRCs in relation to pore size distribution (PSD), changes due to wetting and drying (W–D) cycles were studied in three different tropical soils (Geric Ferralsol, GF; Eutric Nitosol, EN; Rhodic Ferralsol, RF), using three different treatments: T_0 , the control with samples not submitted to W–D cycles; T_3 , samples submitted to three consecutive W–D cycles; T_9 , samples submitted to nine consecutive W–D cycles. Log-normal PSD equations for each treatment were obtained using the S-theory. For the GF soil, the pressure heads separating structural and matrix domains (h_s) were 17.7, 12.2 and 14.7 kPa for T_0 , T_3 , and T_9 , respectively. These values are equivalent to pore radii of 8.4 μm (T_0), 12 μm (T_3), and 10 μm (T_9). For the RF soil, h_s values were 8.5 kPa (T_0), 20.5 kPa (T_3), and 15.1 kPa (T_9), equivalent to radii of 18 μm (T_0), 7.3 μm (T_3), and 9.9 μm (T_9); and finally, for the EN soil, h_s were 18.1 kPa (T_0), 9.1 kPa (T_3), and 13.5 kPa (T_9), equivalent to radii of 8.2 μm (T_0), 16 μm (T_3), and 11 μm (T_9). It was found that the soil structure presented important changes in PSD due to W–D cycles for all the investigated soils. It was also observed that the W–D cycles increased the S_{inf} (slope of SWRC) value for the GF soil for all treatments; S_{inf} did not substantially change in all treatments for the EN soil; S_{inf} decreased between T_0 and T_3 , and T_0 and T_9 for the RF soil. According to the S-theory, it is possible to infer that W–D cycles improved the soil structure of GF, made the RF soil structure worse and did not substantially change the EN soil structure.

© 2008 Elsevier B.V. All rights reserved.

1. Introduction

Soil water retention curves (SWRCs) can be used to estimate pore size distributions (PSDs) (Arya and Paris, 1981; Jury et al., 1991; Kutílek and Nielsen, 1994). They relate soil water contents (θ) to soil water pressure heads (h) or relative soil saturations (S^*).

Information on PSD and its modification due to natural or human processes is very important to characterize induced changes in soil structure and hydraulic properties (Pagliai et al., 1998). Based on their role in water conduction or retention properties, soil pore systems (SPS) can be assumed to be composed of three main pore categories: (1) submicroscopic pores; (2) micropores (divided in matrix or textural and structural pores) or

capillary pores; (3) macropores or non-capillary pores (Kutílek, 2004).

Aggregated soils present differences between textural and structural pores. Textural pores are basically related to the distribution of primary soil particles (sand, silt, and clay) and structural pores are associated to shape, orientation, and position arrangement of soil aggregates (Nimmo, 1997). Textural pores are relatively more stable than structural pores, these last ones being more affected by natural soil processes or human actions as, for instance, agricultural management practices, wetting and drying (W–D) cycles, earthworm activity, and cropping procedures (Zund et al., 1997; Hussein and Adey, 1998; Pillai and McGarry, 1999).

Frequently SWRCs have more than one inflection point, which leads to more than one peak along the curve of PSD. If PSD exhibits two peaks (bi-modal PSD), it represents a typical result for soils with two categories of capillary pores—textural and structural. SWRCs with more than one inflection point are representative of structured soils (Kutílek et al., 2006).

The use of the pore size log-normal distribution model of h , which is derived from the bi-modal PSD (Kosugi, 1994), make it

* Corresponding author at: Departamento de Física, Universidade Estadual de Ponta Grossa, Campus de Uvaranas, Bloco L, Sala 115, Av. Carlos Cavalcanti 4748, C.E.P. 84.030-900 Ponta Grossa, PR, Brazil. Tel.: +55 42 3220 3044; fax: +55 42 3220 3042.

E-mail addresses: lfpires@uepg.br, luizfp@uepg.br, luizfp@gmail.com (L.F. Pires).

possible to characterize changes in SPS due to W–D cycles. Another tool used for the same purpose is based on the shape (slope at the inflexion point, S_{inf}) of the SWRC, which depends on the soil microstructure (Dexter and Birkas, 2004). According to Dexter (2004a,b,c), S_{inf} is related to the sharpness of PSD and it can be used as an index to give indications on soil physical quality.

W–D cycles effects on physical properties of soils have been frequently mentioned in literature (Sartori et al., 1985; Hussein and Adey, 1998; Bresson and Moran, 2003; Timm et al., 2006). Most of the time they cause an irreversible rearrangement of particles inside the matrix frame affecting soil resistance, particle cohesion, internal friction, aggregate size and stability (Rajaram and Erbach, 1999). These cycles can also result in aggregate formation in non-aggregated soils (Newman and Thomasson, 1979).

The objective of this study was to use the log-normal PSD model of h and the S_{inf} index (S-theory) to evaluate effects of W–D cycles on the structure and quality of three Brazilian soils.

2. Material and methods

2.1. Soil sampling

Core samples were collected in Piracicaba, SP, Brazil (22°4'S; 47°38'W; 580 m above sea level), on soil profiles characterized as Geric Ferralsol (GF), Eutric Nitosol (EN), and Rhodic Ferralsol (RF) (Table 1) according to FAO classification (FAO, 1998). According to Koppen's classification, the climate in Piracicaba is a typical Cwa, tropical highland, mesothermal with a dry winter. Average air temperature, rainfall, and relative humidity are 21.2 °C, 1253 mm per year, and 74%, respectively. The dry season covers June–August, July being the driest month. During spring–summer, October–March, intense rainfall (50 mm/h or more) commonly occurs.

Samples of GF were collected in a non-cultivated area covered by grasses and weeds; samples of EN in a coffee field established in 2001; and of RF in a native mixed forest.

Fifteen core samples of each soil type were collected from the soil surface layer (3–7 cm) using aluminum cylinders (3.0 cm high and 4.8 cm in diameter). Details regarding sampling procedures can be found in Pires et al. (2006).

2.2. Wetting and drying (W–D) cycles

Soil samples were saturated by the capillary rise method. Wetting (W) consisted in soaking the samples in a tray with the water level just below the top of the aluminum rings. It was found that 48 h were enough to reach saturation and to minimize entrapped air bubbles in the samples.

A W–D cycle consisted of the following procedure: (1) first the samples were saturated as described previously; (2) thereafter they were partially dried by submitting them to a 400 kPa pressure

in a pressure chamber; finally (3) the samples were saturated once again.

Three treatments were investigated: T_0 , the control, with samples not submitted to W–D cycles; T_3 , samples submitted to three consecutive W–D cycles; T_9 , samples submitted to nine consecutive W–D cycles.

2.3. Water retention characteristics

SWRCs were determined by the traditional method (Richards, 1941), using low- and high-pressure extraction vessels—Soil Moisture Equipment Corporation, which support pressures up to 500 and 1500 kPa, respectively. The SWRC for each treatment was measured for 13 different values of h (1, 3, 6, 9, 10, 30, 50, 90, 120, 150, 300, 500, and 1500 kPa). Five replicates of each soil type were used to generate the mean SWRCs for T_0 , T_3 , and T_9 treatments.

SWRC data (h , θ) were adjusted using the van Genuchten equation (Eq. (1)) with the Mualem restriction ($m = 1 - 1/n$) (van Genuchten, 1980; Mualem, 1986):

$$\theta = \theta_{res} + \frac{\theta_{sat} - \theta_{res}}{[1 + (\alpha h)^n]^m} \quad (1)$$

where θ_{sat} and θ_{res} represent the saturated and residual water contents, respectively; α is the scaling factor for h ; and m and n are parameters related to the shape of the fitted curve. The RETC, Retention Curve software (van Genuchten et al., 1991) was used to fit mean θ and h data for each soil and treatment.

The soil relative saturation was obtained using the following equation:

$$S^* = \frac{\theta - \theta_{res}}{\theta_{sat} - \theta_{res}} \quad (2)$$

Values of θ_{res} for each soil were taken as the water content at 1500 kPa. Data of θ were transformed into S^* and a cubic spline function (Kastanek and Nielsen, 2001) was used to fit the experimental data of S^* versus $\ln h$ resulting a smooth curve.

Water pressure heads were converted to the pore radius (r) using the relation $r = 1490/h$, with r and h given in μm and cm, respectively (Kutílek and Nielsen, 1994). After this transformation $dS^*(\ln h)/d \ln h$ versus $\ln r$ represent the pore size distribution plots.

2.4. Log-normal model and S-theory

Theoretical details about the log-normal model and its application can be found in Kosugi (1994), Kutílek (2004), and Kutílek et al. (2006). Dexter and Bird (2001), using the S-theory, have shown that the water potential at the inflexion point (h_{inf}) in a

Table 1
Some physical and chemical characteristics of the 0–0.10 m layer for the experimental soils

Characteristic	Geric Ferralsol	Soil Eutric Nitosol	Rhodic Ferralsol
Sand (%)	66	24	26
Clay (%)	28	43	48
Silt (%)	6	33	26
Organic matter (g dm^{-3})	16.0	20.2	27.0
Dry bulk density (Mg m^{-3})	1.56	1.62	1.33
Particle density (Mg m^{-3})	2.55	2.68	2.54
K ($\text{mmol}_c \text{ kg}^{-1}$)	2.6	4.3	3.4
Ca ($\text{mmol}_c \text{ kg}^{-1}$)	13.0	29.0	27.0
Mg ($\text{mmol}_c \text{ kg}^{-1}$)	4.0	20.0	15.0
pH (in CaCl_2)	3.9	5.3	4.9

$\ln h$ versus θ plot is given by

$$h_{\text{inf}} = \frac{1}{\alpha} \left(\frac{1}{m} \right)^{1/n} \quad (3)$$

and, as a consequence:

$$\theta_{\text{inf}} = \theta_{\text{res}} + \frac{\theta_{\text{sat}} - \theta_{\text{res}}}{[1 + 1/m]^m} \quad (4)$$

and, as shown by Dexter (2004a), the slope of the water retention curve at the inflexion point is given by

$$S_{\text{inf}} = \frac{-n(\theta_{\text{sat}} - \theta_{\text{res}})}{[1 + 1/m]^{(1+m)}} \quad (5)$$

3. Results and discussion

An increase in θ can be seen near saturation (Fig. 1A), which indicates that the W–D cycles increased soil porosity. At high pressure heads (from 100 to 1500 kPa) the curves for each treatment approximate one each other and for pressures higher than 350 kPa the curves for T_3 and T_9 become similar. All this information indicates that for GF, W–D cycles caused changes in the SWRC essentially near the saturation condition.

For EN samples an opposite behavior was observed (Fig. 1B), once the W–D cycles systematically promoted a decrease in soil porosity. Then, as a whole, the SWRCs of both T_3 and T_9 deviated to lower values of θ at saturation.

In relation to RF (Fig. 1C), initially W–D cycles promoted a soil porosity reduction, more significant for T_3 as related to T_9 . It can also be seen that it becomes more difficult to extract water from the samples submitted to W–D cycles since the remaining θ of the samples (soil water content for pressures above 10 kPa) decreased as compared to T_0 , for both treatments.

Some authors have reported that compaction by natural or artificial processes reduces soil water storage capacity, mainly due to a reduction of the amount of large pores followed by a rising amount of small pores. As a consequence, the SWRCs of compacted soils are mainly altered at low pressure heads (from 0 to 10 kPa) and at high pressure heads (from 300 to 1500 kPa) (Kutílek and Nielsen, 1994; Ferrero and Lipiec, 2000). Compacted soils present flatten SWRCs with a reduction of the S_{inf} (Dexter, 2004a; Assouline et al., 1997; Hayashi et al., 2006).

The adjusted parameters to the SWRCs presented in Fig. 1 had determination coefficients (R^2) close to unit, indicating that the adjustment of the proposed interpolation equation to the experimental data was excellent (Table 2).

The spline function curves of S^* versus $\ln h$ are presented in Fig. 2 and the derivative curves $dS^*(\ln h)/d \ln h$ in Fig. 3.

W–D cycles changed S^* and $dS^*(\ln h)/d \ln h$ characteristics for all soils (Fig. 2). For GF (Figs. 2A and 3A), T_0 and T_3 presented a tri-modal PSD while T_9 exhibited a tetra-modal PSD. Nevertheless, Kastanek and Nielsen (2001) reported that sometimes a multi-modal PSD can be originated from the spline adjustment procedure itself, however, tetra-modal PSD was already observed for soils submitted to different tillage treatments (Lipiec et al., 2006). Changes in PSD due to different treatments occur mainly for pore radia ranging from 0.63 to 2.3 μm , 3.3 to 10 μm , and 12 to 130 μm , the largest modifications being observed in the last mentioned pore range (structural domain).

W–D cycles clearly raised the amount or the size of large pores (10–500 μm) for GF samples (Fig. 3A). The peak associated to the structural domain for GF, corresponds approximately to pores of 25 μm (T_0), 32 μm (T_3), and 35 μm (T_9) and the W–D cycles imposed to the samples defined it more clearly. In the matrix

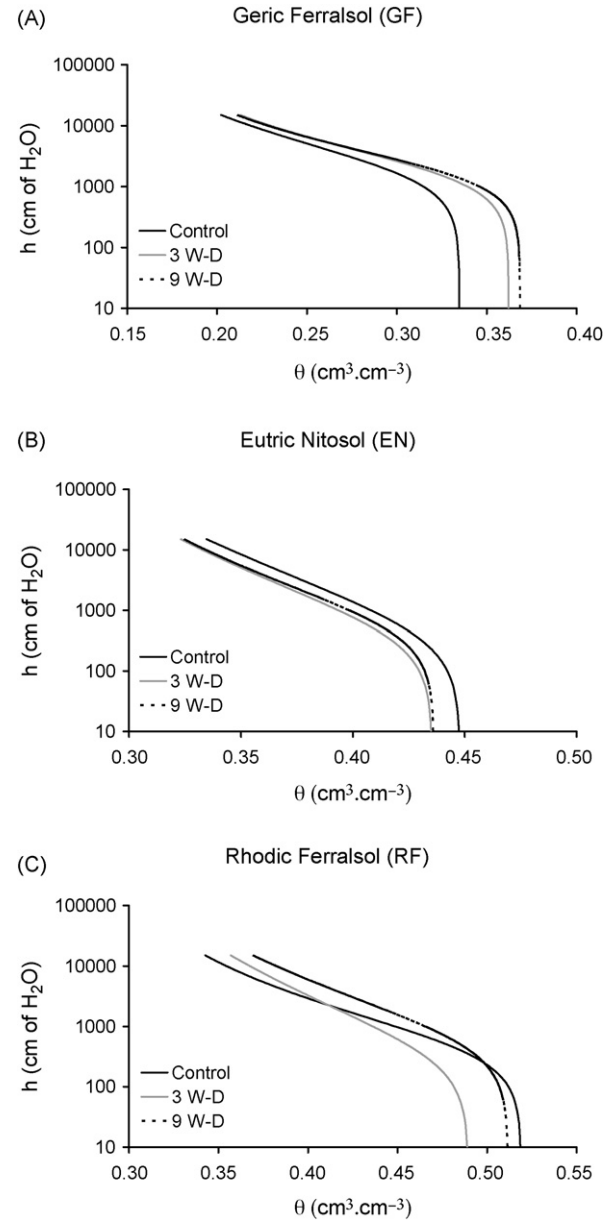


Fig. 1. Soil water retention curves (SWRCs) of the soils used after the application of wetting and drying (W–D) cycles; h and θ represent water pressure head and soil water content, respectively.

domain (from about 0.1 to 18 μm) T_3 and T_9 exhibited only slight differences in relation to T_0 .

The pore radius that separates the structural from the matrix domain was estimated at the minimum of the $dS^*(\ln h)/d \ln h$ curve. For GF, these minimum values (h_s) occurred at 8.4 μm (T_0), 12 μm (T_3), and 10 μm (T_9). These radia correspond to pressure values of 17.7 kPa (T_0), 12.2 kPa (T_3), and 14.7 kPa (T_9), respectively.

Tri-modal PSDs were found for all treatments of EN (Fig. 3B). Control samples presented well-defined $dS^*(\ln h)/d \ln h$ peaks that were modified after three and nine W–D cycles. Even being produced in both domains (matrix and structural), major changes in PSD for EN occurred in the matrix domain. Peaks located in the structural domain were found at pore radia of about 77 μm (T_0), 44 μm (T_3), and 39 μm (T_9). Values of h_s for these samples were found at 8.5 kPa (T_0), 20.5 kPa (T_3), and 15.1 kPa (T_9), which are equivalent to pore radia of 18 μm (T_0), 7.3 μm (T_3), and 9.9 μm (T_9), respectively.

A quasi bi-modal PSD was found for T_0 of RF (Fig. 3C) and W–D cycles changed it to tri-modal (T_3 and T_9). Both matrix and structural domains presented important alterations regarding PSD for this type of soil. In the matrix domain T_0 and T_3 exhibited only slight differences in relation to T_9 , however the opposite occurred among treatments in the structural domain. There was a decrease in the peak associated to pores located in this domain. The peak position was also slightly deviated to smaller pore values. The peak positions were found at $56 \mu\text{m}$ (T_0), $42 \mu\text{m}$ (T_3), and $48 \mu\text{m}$ (T_9). The results of h_s obtained for RF were 18.1 kPa (T_0), 9.1 kPa (T_3), and 13.5 kPa (T_9), which are equivalent to pore radii of $8.2 \mu\text{m}$ (T_0), $16 \mu\text{m}$ (T_3), and $11 \mu\text{m}$ (T_9), respectively. The results of PSD analysis allow concluding that the application of W–D cycles raised the amount of large pores for GF and EN and decreased it for RF.

All soils with treatments presented h_s values ranging between 8.5 and 20.5 kPa , which are equivalent to pore radii ranging from 7.3 to $18 \mu\text{m}$.

Tuller and Or (2002) and Kutílek et al. (2006) found h_s values ranging between 0.1 and $10.9 \mu\text{m}$. Nevertheless, Kutílek et al. (2006) and Hajnos et al. (2006) mention that depending on the soil type and management, the boundary between soil pore categories can be strongly variable.

In order to compare the effect of three and nine W–D cycles, Fig. 4 shows differences between $dS^*/d \ln h$ curves for soil samples submitted to these treatments and their respective control samples.

It can be seen between treatments that nine W–D cycles caused more pronounced changes in the $dS^*/d \ln h$ behavior for GF (Fig. 4A), the most important changes occurring in the structural domain. The nine W–D cycle treatment produced major changes in the $dS^*/d \ln h$ and S^* behaviors for EN (Figs. 2B and 4B). However, the most significant changes were found in the matrix domain. For RF (Fig. 4C), while T_3 produced larger modifications in the structural domain, T_9 produced larger modifications in the matrix domain.

Some soil physical properties as, for example, total porosity, stress state and energy state may change due to W–D cycles (Baumgartl, 1998). Pires et al. (2008) showed that small alterations in total volume of soil core samples resulted from the application of W–D cycles. It is mainly caused by stresses originated from capillary forces, which increase with soil drainage. As a consequence, each re-wetting process leads to definitive modifications in the soil structure.

To characterize modifications introduced in soil structure by W–D cycles, some observations based on S-theory were made to investigate the shape of the obtained SWRCs (Dexter, 2004a). According to this theory, the S_{inf} of a SWRC is a quantity related to soil microstructure and it can be used as a parameter for soil physical quality characterization. The results of the S_{inf} and θ_{inf} (see Eqs. (4) and (5)) obtained for all soils and treatments are given in Table 3.

Table 2

SWRC parameters obtained for the van Genuchten equation for the soils submitted to T_0 (samples not submitted to W–D cycles), T_3 (samples submitted to three W–D cycles), and T_9 (samples submitted to nine W–D cycles) treatments

Parameters	GF ^a			EN ^a			RF ^a		
	T_0	T_3	T_9	T_0	T_3	T_9	T_0	T_3	T_9
θ_{sat} ($\text{cm}^3 \text{cm}^{-3}$)	0.335	0.362	0.369	0.448	0.435	0.436	0.519	0.490	0.512
θ_{res} ($\text{cm}^3 \text{cm}^{-3}$)	0.111	0.136	0.144	0.113	0.184	0.222	0.263	0.197	0.226
α (cm^{-1})	0.0490	0.0516	0.0496	0.2104	0.2245	0.1645	0.1992	0.2773	0.1519
n	1.440	1.518	1.593	1.119	1.168	1.228	1.344	1.162	1.220
m	0.306	0.341	0.372	0.106	0.144	0.186	0.256	0.139	0.180
R^2	0.996	0.999	0.998	0.995	0.998	0.999	0.995	0.998	0.996

^a GF, EN, and RF represent Geric Ferralsol, Eutric Nitosol, and Rhodic Ferralsol, respectively.

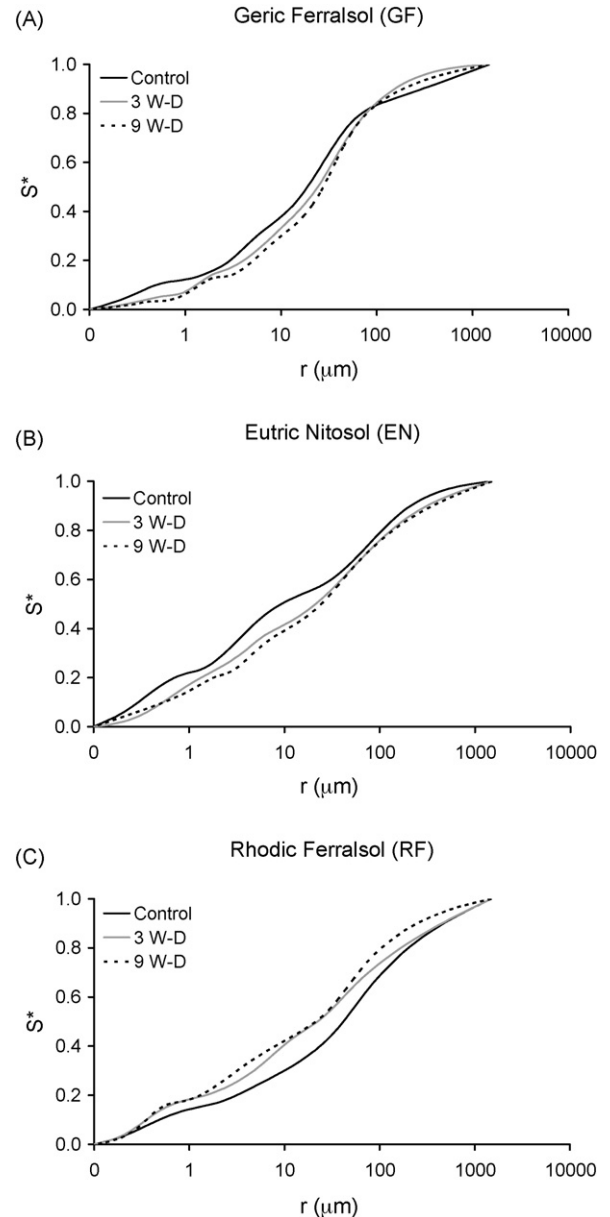


Fig. 2. Relative soil saturation (S^*) curves versus water pressure head (h) obtained using a smooth cubic spline adjustment after application of wetting and drying (W–D) cycles.

Dexter and Birkas (2004) related the S_{inf} to soil clay and silt contents, soil bulk density, soil organic matter content, and soil water content at saturation. S_{inf} values here obtained were compared to those found in the previously mentioned work (Table 4).

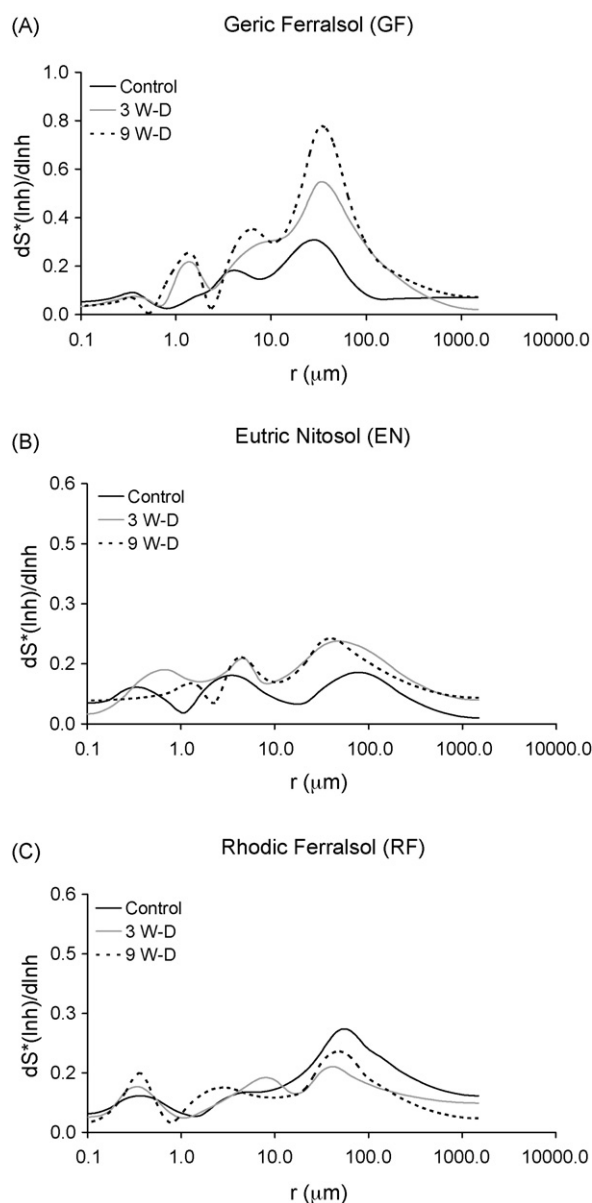


Fig. 3. The derivative curves of S^* ($dS^*(\ln h)/d \ln h$) versus the pore radius (r) after application of wetting and drying (W–D) cycles.

Related to the clay content, only EN presented S_{inf} values in accordance to predicted ones; associated to silt content, the S_{inf} determined for each investigated soil agreed very well with the predicted ones. In relation to OM and ρ_b only GF presented S_{inf} values in agreement with the predicted ones. In relation to θ_{sat} both GF and RF had S_{inf} values in accordance to predicted ones (Dexter and Birkas, 2004).

Table 3

S_{inf} and θ_{inf} values for three different Brazilian soil texture classes after application of wetting and drying cycles

Parameter	GF ^a			EN ^a			RF ^a		
	T_0^b	T_3^b	T_9^b	T_0	T_3	T_9	T_0	T_3	T_9
θ_{inf} ($\text{cm}^3 \text{cm}^{-3}$)	0.254	0.278	0.282	0.374	0.371	0.374	0.433	0.415	0.430
S_{inf}	0.0485	0.0549	0.0597	0.0281	0.0274	0.0292	0.0466	0.0310	0.0379

^a GF, EN, and RF represent Geric Ferralsol, Eutric Nitosol, and Rhodic Ferralsol, respectively.

^b T_0 , the control with samples not submitted to wetting and drying (W–D) cycles; T_3 , samples submitted to three consecutive W–D cycles, and T_9 , samples submitted to nine consecutive W–D cycles.

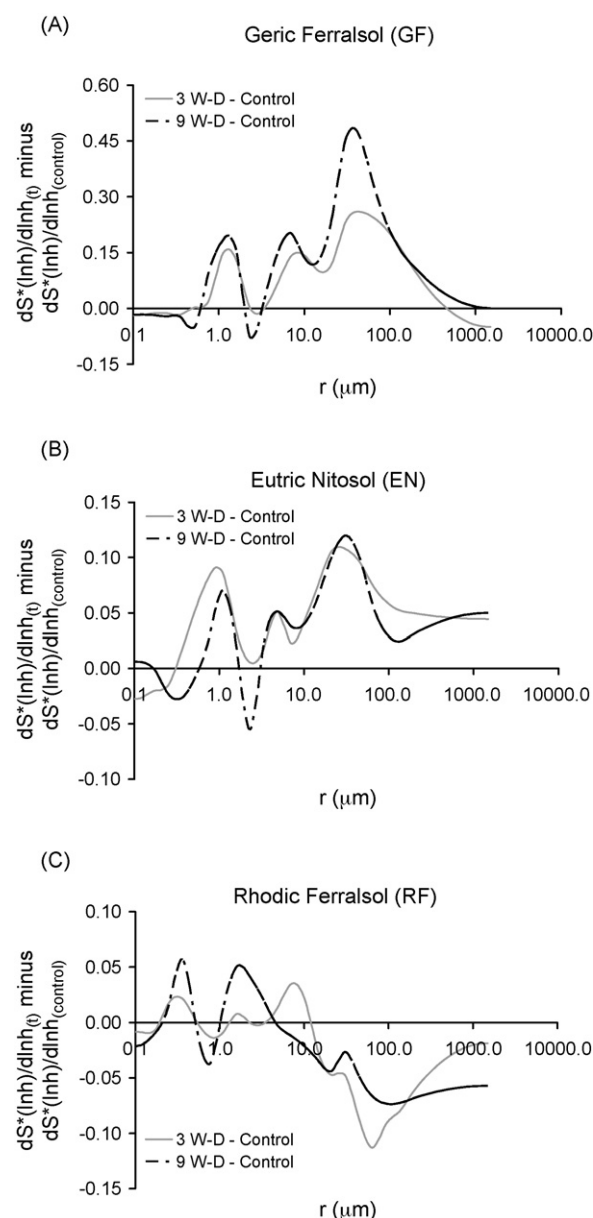


Fig. 4. Differences of the derivative S^* curves ($dS^*(\ln h)/d \ln h$) shown in Fig. 3 between T_0 (the control with samples not submitted to wetting and drying (W–D) cycles) and T_3 (samples submitted to three consecutive W–D cycles) treatments ($dS^*(\ln h)/d \ln h$ T_3 curve minus $dS^*(\ln h)/d \ln h$ control curve) and T_0 and T_9 (samples submitted to nine consecutive W–D cycles) ($dS^*(\ln h)/d \ln h$ T_9 curve minus $dS^*(\ln h)/d \ln h$ control curve), respectively.

For this study, changes in the S_{inf} were also utilized to predict soil physical quality variations due to the application of W–D cycles. Table 3 shows an increase in the S_{inf} for GF due to W–D cycles. For EN, the S_{inf} was practically the same among treatments

Table 4
Predicted values of S_{inf} according with the work of Dexter and Birkas (2004)

Soil type	GF		EN		RF	
	$S_{\text{inf}}^{\text{a}}$	$P (\%)^{\text{b}}$	S_{inf}	$P (\%)$	S_{inf}	$P (\%)$
Clay (%)	0.0351	38	0.0293	4	0.0289	61
OM (%)	0.0656	26	0.0423	34	0.0323	44
ρ_b (g cm $^{-3}$)	0.0522	7	0.0867	68	0.0294	58
θ_{sat} (cm 3 cm $^{-3}$)	0.0518	6	0.0496	43	0.0514	9

^a Predicted values of S_{inf} were determined based on a first order exponential decay adjustment for $S_{\text{inf}} \times \rho_b$ plot and a second-order exponential decay adjustment for $S_{\text{inf}} \times \text{Clay}$; $S_{\text{inf}} \times \text{OM}$; and $S_{\text{inf}} \times \theta_{\text{sat}}$ plots of data obtained by Dexter and Birkas (2004).

^b P represents the percentual deviation.

and for RF it decreases from T_0 to T_3 and T_9 . These results show larger differences in the SWRCs and SPS for GF and RF as compared to EN.

According to Dexter (2004a), soil compaction reduces the S_{inf} and large values are an index of good soil quality, indicating the presence of structural pores. On the other hand, soils with poor physical quality present small values of S_{inf} . Based on this information, it can be inferred that the structure of GF was improved with the application of W–D cycles and the opposite result was observed for RF. EN samples did not present any significant change in soil structure based on S_{inf} values.

Acknowledgements

To the Araucária Foundation (grant no. 10193), the Fund Paraná/SETI, Paraná State Government, and the National Research Foundation (CNPq) both of Brazil, for financial support.

References

- Arya, L.M., Paris, J.F., 1981. Physicoempirical model to predict the soil moisture characteristic from particle-size distribution and bulk density data. *Soil Sci. Soc. Am. J.* 45, 1023–1030.
- Assouline, S., Tavares-Filho, J., Tessier, D., 1997. Effect of compaction on soil physical and hydraulic properties: experimental results and modeling. *Soil Sci. Soc. Am. J.* 61, 390–398.
- Baumgartl, Th., 1998. Physical soil properties in specific fields of application especially in anthropogenic soils. *Soil Till. Res.* 47, 51–59.
- Bresson, L.M., Moran, C.J., 2003. Role of compaction versus aggregate disruption on slumping and shrinking of repacked hardsetting seedbeds. *Soil Sci.* 168, 585–594.
- Dexter, A.R., Bird, N.R.A., 2001. Methods for predicting the optimum and the range of water contents for tillage based on the water retention curve. *Soil Till. Res.* 57, 203–212.
- Dexter, A.R., 2004a. Soil physical quality. Part I. Theory, effects of soil texture, density, and organic matter, and effects on root growth. *Geoderma* 120, 201–214.
- Dexter, A.R., 2004b. Soil physical quality. Part II. Friability, tillage, tilth and hard-setting. *Geoderma* 120, 215–225.
- Dexter, A.R., 2004c. Soil physical quality. Part III. Unsaturated hydraulic conductivity and general conclusions about S-theory. *Geoderma* 120, 227–239.
- Dexter, A.R., Birkas, M., 2004. Prediction of the soil structures produced by tillage. *Soil Till. Res.* 79, 233–238.
- FAO, 1998. World Reference Base for Soil Resources. FAO, ISRIC and ISSS, Rome, Italy.
- Ferrero, A., Lipiec, J., 2000. Determining the effect of trampling on soils in hillslope-woodlands. *Int. Agrophys.* 14, 9–16.
- Hayashi, Y., Ken'ichirou, K., Mizuyama, T., 2006. Changes in pore size distribution and hydraulic properties of forest soil resulting from structural development. *J. Hydrol.* 331, 85–102.
- Hajnos, M., Lipiec, J., Swieboda, R., Sokolowska, Z., Witkowska-Walczak, B., 2006. Complete characterization of pore size distribution of tilled and orchard soil using water retention curve, mercury porosimetry, nitrogen adsorption, and water desorption methods. *Geoderma* 135, 307–314.
- Hussein, J., Adey, M.A., 1998. Changes in microstructure, voids and b-fabric of surface samples of a Vertisol caused by wet/dry cycles. *Geoderma* 85, 63–82.
- Jury, A.W., Gardner, W.R., Gardner, W.H., 1991. *Soil Physics*. John Wiley & Sons, New York, p. 328.
- Kastanek, F.J., Nielsen, D.R., 2001. Description of soil water characteristics using a cubic spline interpolation. *Soil Sci. Soc. Am. J.* 65, 279–283.
- Kosugi, K., 1994. Three-parameter lognormal distribution model for soil water retention. *Water Resour. Res.* 30, 891–901.
- Kutílek, M., Nielsen, D.R., 1994. *Soil Hydrology*. Catena Verlag, Germany.
- Kutílek, M., 2004. Soil hydraulic properties as related to soil structure. *Soil Till. Res.* 79, 175–184.
- Kutílek, M., Jendele, L., Panayiotopoulos, K.P., 2006. The influence of uniaxial compression upon pore size distribution in bi-modal soils. *Soil Till. Res.* 86, 27–37.
- Lipiec, J., Kus, J., Slowin'ska-Jurkiewicz, A., Nosalewicz, A., 2006. Soil porosity and water infiltration as influenced by tillage methods. *Soil Till. Res.* 89, 210–220.
- Mualem, Y., 1986. Hydraulic conductivity of unsaturated soils: prediction and formulas. In: Klute, A. (Ed.), *Methods of Soil Analysis. I. Physical and Mineralogical Methods*, vol. 9. ASA, SSSA, Madison, pp. 799–823.
- Newman, A.C.D., Thomasson, A.J., 1979. Rothamsted studies of soil structure. III. Pore size distributions and shrinkage processes. *J. Soil Sci.* 30, 415–439.
- Nimmo, J.R., 1997. Modeling structural influences on soil water retention. *Soil Sci. Soc. Am. J.* 61, 712–719.
- Pagliai, M., Rousseva, S., Vignozzi, N., Piovaneli, C., Pellegrini, S., Miclaus, N., 1998. Tillage impact on soil quality. I. Soil porosity and related physical properties. *Ital. J. Agron.* 2, 11–20.
- Pillai, U.P., McGarry, D., 1999. Structure repair of a compacted Vertisol with wet-dry cycles and crops. *Soil Sci. Soc. Am. J.* 63, 201–210.
- Pires, L.F., Bacchi, O.O.S., Dias, N.M.P., 2006. Gamma-ray beam attenuation to assess the influence of soil texture on structure deformation. *Nukleonika* 51, 125–129.
- Pires, L.F., Cooper, M., Cássaro, F.A.M., Reichardt, K., Bacchi, O.O.S., Dias, N.M.P., 2008. Micromorphological analysis to characterize structure modifications of soil samples submitted to wetting and drying cycles. *Catena* 72, 297–304.
- Rajaram, G., Erbach, D.C., 1999. Effect of wetting and drying on soil physical properties. *J. Terramech.* 36, 39–49.
- Richards, L.A., 1941. A pressure-membrane extraction apparatus for soil solution. *Soil Sci.* 51, 377–386.
- Sartori, G., Ferrari, G.A., Pagliai, M., 1985. Changes in soil porosity and surface shrinkage in a remolded, saline clay soil treated with compost. *Soil Sci.* 139, 523–530.
- Timm, L.C., Pires, L.F., Roveratti, R., Arthur, R.C.J., Reichardt, K., Oliveira, J.C.M., Bacchi, O.O.S., 2006. Field spatial and temporal patterns of soil water content and bulk density changes. *Sci. Agric.* 63, 55–64.
- Tuller, M., Or, D., 2002. Unsaturated hydraulic conductivity of structured porous media. A review. *Vadose Zone J.* 1, 14–37.
- van Genuchten, M.Th., 1980. A closed-form equation for predicting the hydraulic conductivity of unsaturated soils. *Soil Sci. Soc. Am. J.* 44, 892–898.
- van Genuchten, M.Th., Liej, F.J., Yates, S.R., 1991. The RETC code for quantifying the hydraulic functions of unsaturated soils. USDA, US Salinity Laboratory, Document EPA/600/2-91/065, Riverside, CA, USA.
- Zund, P.R., Pillai-McGarry, U., McGarry, D., Bray, S.G., 1997. Repair of a compacted Oxisol by the earthworm *Pontoscolex corethrurus* (Glossoscolecidae, Oligochaeta). *Biol. Fert. Soils* 25, 202–208.